Nonlinear Dyn (2019) 97:1567–1580
https://doi.org/10.1007/s11071-019-05073-8

ORIGINAL PAPER

Adaptive backstepping control for flexible-joint manipulator using interval type-2 fuzzy neural network approximator

Songyi Dian · Yi Hu · Tao Zhao · Jixia Han

Received: 19 January 2019 / Accepted: 14 June 2019 / Published online: 22 June 2019

Abstract In this paper, an adaptive backstepping controller based on interval type-2 fuzzy neural network (IT2FNN) approximator is proposed for flexible-joint manipulator with mismatched uncertainties. Backstepping control has the ability to deal with the mismatched problem, and IT2FNN approximator can be utilized to approximate unknown nonlinear functions. Through the Lyapunov stability analysis, all the signals in the closed-loop system are guaranteed to be ultimately bounded. Simulation results show that the tracking error of the proposed controller can be reduced to arbitrarily small values, and the tracking performance is better than the adaptive backstepping controllers based on type-1 fuzzy neural network approximator and neural network approximator.

Keywords Flexible-joint manipulator · Adaptive backstepping controller · Neural network · Interval type-2 fuzzy

1 Introduction

Over the past three decades, flexible-joint manipulator has attracted a great deal of interests owing to its obvious superiority of small actuators, high precision and low energy consumption [1–7]. In contrast to the rigid manipulator, flexible-joint manipulator possess flexibility, high security and low rate of damages [8–10]. In 1989, Spong derived a reduced-order model of the manipulator which was the fist simplified dynamic model and they presented the first adaptive control law for flexible-joint robots [11,12]. In the modeling and control, the flexible-joint manipulator presents serious problems because of the inherent highly coupling, nonlinearity and model uncertainty. Therefore, it improves the difficulty of the controller design which has led to a great deal of research using advanced control theory to design more appropriate controllers [2,13–15].

At present, backstepping approach is one of the most commonly used design methods for solving nonlinear systems. In [16], a new adaptive backstepping controller was proposed to the adaptive tracking problem in uncertain flexible-joint manipulator system. [17] presented an adaptive sliding control method using a backstepping-like design for single-link flexible-joint robot. However, it is difficult to obtain complete or partial machine parameters in many practical applications, and motion in robot is a complicated nonlinear process that is hard to model as a linear-in-the-parameter process. The function approximation technique has the great advantages to deal with this issue, which does not require the system dynamics to be exactly known [18–20]. Adaptive backstepping controllers combined with several universal approximators have been successfully presented to control the uncertain manipulator system, such as recurrent neural net-

S. Dian · Y. Hu · T. Zhao (✉) · J. Han
College of Electrical Engineering and Information Technology, Sichuan University, Chengdu 610065, China
e-mail: zhaotaozhaogang@126.com

works [21], self-recurrent wavelet neural network [22], neural networks [23–25] and fuzzy system [26,27]. With the advent of the fuzzy set theory proposed by Zadeh (1965), the fuzzy system was proven to be an effective approach for investigating a bank of complex nonlinear control design problems [28–30]. The type-1 fuzzy model offers a general framework for nonlinear system analysis and controller synthesis [31]. However, due to crisp antecedents and consequents of the rule base, type-1 fuzzy system (T1FS) cannot efficiently handle the uncertainties. Interval type-2 fuzzy system (IT2FS) was widely applied to many practical applications and can obtain better performance for highly nonlinear systems with various uncertainties than T1FS [32–35]. An improved social spider optimization algorithm was proposed to adjust the predecessor parameters of general type-2 fuzzy system (GT2FS) in [36], but one of the important limitations is that the computational cost of the proposed GT2FS is increased in the high-dimensional problems. Due to the simplicity and efficiency of the IT2FS, it is very valuable to use the IT2FS to handle highly nonlinearity of manipulator system in this paper.

IT2FS can improve the system's ability to deal with uncertainties and approximate uncertain unknown functions effectively. [37] solved the globally stable adaptive backstepping control based on IT2FS for a class of nonlinear systems. In [38], backstepping and IT2FS were combined in a unified controller for induction machine. An adaptive backstepping robust control approach based on IT2FS was proposed for uncertain multi-inputs multi-outputs chaotic system in [39]. IT2FNN has potential to improve approximation accuracy, but there are very few researches to design adaptive controller for flexible-joint manipulators using IT2FNN approximator. In [40,41], sliding mode control methods with the IT2FS approximator for flexible-joint manipulator were proposed. In the current rare attempts in developing IT2FNN approximator, high time consumption of the iterative K–M algorithm is still a problem that cannot be ignored. In the previous papers on IT2FS approximator, the iterative K–M algorithm is used to rearrange the rule's consequent weights in ascending order and find the left and right crossover points [42]. However, high computational complexity and high time consumption of the iterative K–M algorithm in type-reduction of IT2FS make it very hard to be used in practical applications [43]. Therefore, improving the type-reduction algorithm has always been the focus of researchers. The adaptive control factors q_l and q_r were proposed in [44], instead of finding the left and right crossover points in the iterative K–M algorithms. Then, in 2017, Bibi et al. [45] replaced K–M algorithms by the adaptive modulation factor α between the upper output y_r and the lower output y_l in the IT2FNN. The adaptive modulation factor improves the practicability of the algorithm. In this paper, the adaptive modulation factor α is applied to IT2FNN approximator and effectively overcomes computational complexity and high time consumption. To the best of the authors knowledge, improved IT2FNN approximator has not yet been investigated for flexible-joint manipulator, thereby leaving room for continued promotion. This study is the first attempt to apply adaptive modulation factor into IT2FNN approximator to design adaptive backstepping controller for flexible-joint manipulator with uncertain dynamics. Thus, the tracking performance of the system can be improved by the proposed method.

Based on the above discussion, the motivation of this study is triggered. An adaptive backstepping control method based on IT2FNN approximator for flexible-joint manipulator is proposed. Using Lyapunov stability theory, all the signals in the closed-loop system are guaranteed to be ultimately bounded. Compared to the existing works, the proposed approach does not require the unknown parameters to be linear parameterizable and the tracking error can be reduced to arbitrarily small values. The main contributions of this paper are as follows: (1) This paper is the first attempt in developing the adaptive modulation factor α into IT2FNN approximator to control flexible-joint manipulators with mismatched uncertainties. (2) We devise the adaptive law of adaptive modulation factor α and the adaptive parameters from Lyapunov stability analysis. The adaptive modulation factor can be iteratively updated, and thus the ability of adaptive ponderation between the upper output y_r and the lower output y_l can be improved. (3) The proposed controller can guarantee not only the stability of manipulator system but also the boundedness of all the signals in the closed-loop system. (4) Compared with the T1FNN and the NN approximator, simulation results demonstrate that the proposed scheme has better steady-state performance, less fluctuation and higher approximation accuracy.

The rest of paper is organized as follows. The problems formulation is presented in Sect. 2. Section 3

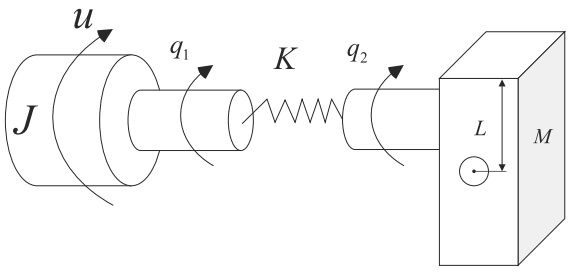

Fig. 1 Schematic of flexible-joint manipulator model

describes the IT2FNN approximator. In Sect. 4, we derive the proposed controller and verify stability of the closed loop using Lyapunov approach. Section 5 presents the feasibility and the effectiveness of proposed controller for flexible-joint manipulator by comparing with the others control methods. Finally, conclusions are drawn in Sect. 6.

2 Problem formulation

This section is referenced from [17]. A schematic model of a single-link flexible-joint manipulator is shown in Fig. 1. We assume that its joint can only be deformed when rotating in a vertical plane in the direction of joint rotation. The operating mechanism of the flexible-joint manipulator is that the motor shaft and the rigid link are, respectively, driven by the motor and spring to rate. Assuming that the viscous damping is ignored and the states are measurable, its dynamic equation is given by

$$\begin{cases} I\ddot{q_1} + MgL\sin q_1 + K(q_1 - q_2) = 0 \\ J\ddot{q_2} + K(q_2 - q_1) = u \end{cases} \tag{1}$$

where $q_1 \in R^n$ and $q_2 \in R^n$ are the angular displacements of flexible-joint link and motor, K is the spring stiffness of joints, $u \in R^n$ is the external input, which is the torque delivered by the motor, I and J are, respectively, the moment of inertia of flexible-joint link and the motors, M is the mass of flexible-joint link, and L is the length between the center of gravity of the manipulator and flexible-joints.

We define $x_1 = q_1, x_2 = \dot{q_1}, x_3 = q_2, x_4 = \dot{q_2}$ (1) can be rewritten as the following state-spaced representation

$$\begin{cases} \dot{x_1} = x_2 \\ \dot{x_2} = -\frac{1}{I}(MgL\sin(x_1) + K(x_1 - x_3)) \\ \dot{x_3} = x_4 \\ \dot{x_4} = \frac{1}{J}(u + K(x_1 - x_3)) \end{cases} \tag{2}$$

where $x_i \in R^n, i = 1, 2, 3, 4$ are state variables and $y = x_1$ is the link angular displacement. Considering a single-link flexible-joint manipulator with mismatched uncertainties, the above model cannot be available. Since the robot is basically a link powered by the electric motor through a twisted spring, we can represent it as a cascade of two subsystems: link dynamics and the motor dynamics. The control input is in the subsystem describing the motor dynamics, and its output is coupled to another subsystem with the spring and link dynamics. Therefore, we can write (1) as a simplified system equation

$$\begin{cases} \dot{x_1} = x_2 \\ \dot{x_2} = x_3 + g(x) \\ \dot{x_3} = x_4 \\ \dot{x_4} = f(x) + mu \end{cases} \tag{3}$$

It is obvious that $g(x) = -x_3 - MgL\sin(x_1)/I - K(x_1 - x_3)/I$, $f(x) = K(x_1 - x_3)/J, m = 1/J$. We assume that $g(x)$, $f(x)$ and m are unknown constants where the lower bound of m is known and satisfies $m \geq \underline{m}$ and $\underline{m} > 0$. An adaptive backstepping controller with fuzzy approximation is designed to desired trajectory tracking. IT2FNN is utilized to approximate unknown nonlinear functions.

3 IT2FNN approximator

This section introduces an IT2FNN approximator, which can obtain a very accurate and robust approximation. The architecture of IT2FNN is shown in Fig. 2. IT2FNN has obvious advantages of handling uncertainties and approximating unknown nonlinear functions by using lower and upper membership functions. IT2FNN can be thought as consisting of two parts: one part contains some IF-THEN rules, and the second part is the fuzzy inference engine.

Each rule in the IT2FNN approximator is presented in the following form:

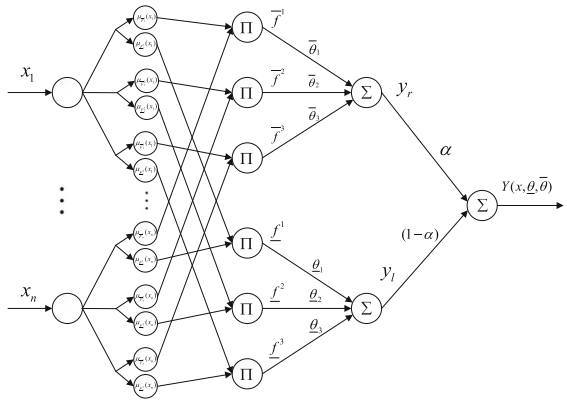

Fig. 2 Architecture of IT2FNN

$$\mathbb{R}^k : \text{if } x_1 \ is \ \hat{F}_1^k \text{ and } \ldots \text{ and } x_n \text{ is } \hat{F}_n^k \quad \text{then } y \text{ is } \theta_k \quad k = 1, \ldots, N \tag{4}$$

where $x_1, x_2, \ldots, x_n$ are the input variables and y is the output variable. N is the total number of fuzzy rules. $\hat{F}_i^k, i = 1, 2, \ldots, n, k = 1, 2, \ldots, N$, are interval type-2 fuzzy antecedent. $\theta_k = [\underline{\theta}_k, \overline{\theta}_k]$ represents the lower and the upper singleton consequent type-2 fuzzy sets. Mathematical function of each operator are described as follows.

For an input vector $x = [x_1, x_2, \ldots, x_n]$, using the singleton fuzzifier and product t-norm, the lower and upper bounds of the firing the kth rule φ^k strength can be computed as follows:

$$\varphi^k = [\underline{f}^k, \overline{f}^k], \quad k = 1, 2, \ldots, N \tag{5}$$

where:

$$\begin{cases} \underline{f}^k = \mu_{\underline{F}_1^k}(x_1) * \cdots * \mu_{\underline{F}_i^k}(x_i) \\ \overline{f}^k = \mu_{\overline{F}_1^k}(x_1) * \cdots * \mu_{\overline{F}_i^k}(x_i) \end{cases} \tag{6}$$

in which $\mu_{\underline{F}_i^k}(x_i)$ and $\mu_{\overline{F}_i^k}(x_i)$, respectively, are the lower membership function and the upper membership function. Then, the type-reduction converts the interval type-2 fuzzy sets to an interval set. Finally, defuzzifier maps the interval set into a crisp output.

There are many methods of designing the type-reduction of interval type-2 fuzzy sets. The most common method is the center-of-sets type-reduction, which can be expressed by:

$$Y_{\text{COS}}(x) = \frac{\sum_{k=1}^N \varphi^k(x_i)\theta_k}{\sum_{k=1}^N \varphi^k(x_i)} = [y_l, y_r] \tag{7}$$

where y_l and y_r are computed as follows:

$$y_l = \frac{\sum_{k=1}^N \underline{f}^k \underline{\theta}_k}{\sum_{k=1}^N \underline{f}^k} = \sum_{k=1}^N \underline{\xi}^k \underline{\theta}_k = \underline{\xi}(x)\underline{\theta}^T \tag{8}$$

and

$$y_r = \frac{\sum_{k=1}^N \overline{f}^k \overline{\theta}_k}{\sum_{k=1}^N \overline{f}^k} = \sum_{k=1}^N \overline{\xi}^k \overline{\theta}_k = \overline{\xi}(x)\overline{\theta}^T \tag{9}$$

where $\underline{\theta} = [\underline{\theta}_1, \underline{\theta}_2, \ldots, \underline{\theta}_N]$ and $\overline{\theta} = [\overline{\theta}_1, \overline{\theta}_2, \ldots, \overline{\theta}_N]$ are the adjustable parameters, $\underline{\xi}(x) = [\underline{\xi}^1, \underline{\xi}^2, \ldots, \underline{\xi}^k]$ and $\overline{\xi}(x) = [\overline{\xi}^1, \overline{\xi}^2, \ldots, \overline{\xi}^k]$ are the fuzzy basis functions that are computed as follows:

$$\underline{\xi}^k = \frac{\underline{f}^k}{\sum_{p=1}^N \underline{f}^p}, \overline{\xi}^k = \frac{\overline{f}^k}{\sum_{p=1}^N \overline{f}^p} \tag{10}$$

K–M and EIASC iterative algorithms can determine some crossover points, which combine the lower output y_l and the upper output y_r. But it consumes a lot of time in iterative process, especially for real-time applications. An adaptive factor α is proposed to obtain an adaptive modulation between y_l and y_r, which can overcome those drawbacks of such iterative algorithm, including high time-consuming and low accuracy-calculating [45].

The defuzzified output $Y(x, \underline{\theta}, \overline{\theta})$ is computed as follows:

$$Y(x, \underline{\theta}, \overline{\theta}) = \alpha y_r + (1 - \alpha) y_l \tag{11}$$

Substituting (8) and (9) into (11), we get

$$Y(x, \underline{\theta}, \overline{\theta}) = \alpha \overline{\xi}(x)\overline{\theta}^T + (1 - \alpha)\underline{\xi}(x)\underline{\theta}^T \tag{12}$$

4 Controller design

In this section, an adaptive backstepping controller with the IT2FNN approximator is proposed for a flexible-joint manipulator with mismatched uncertainties.

4.1 Backstepping controller

In the process of backstepping, at each recursive step, virtual controllers $x_{id}, i = 2, \ldots, m$, are designed to force errors $e_{i-1} = x_{i-1} - x_{(i-1)d}$ as small as possible. The final virtual controller x_{id} is the part of actual controller u. An actual controller for u is used to minimize the error between x_m and x_{md} to be as much as possible. The design of the controller is divided into several steps.

Step 1 Define $e_1 = x_1 - x_{1d}$ and let $x_{1d} = y_d$. We get

$$\dot{e}_1 = \dot{x}_1 - \dot{x}_{1d} = x_2 - \dot{x}_{1d} \tag{13}$$

Define $e_2 = x_2 - x_{2d}$ and a virtual controller x_{2d}.

$$x_{2d} = \dot{x}_{1d} - k_1 e_1 \tag{14}$$

where k_1 is a positive constant.

Then, (13) can be rewritten as:

$$\dot{e}_1 = e_2 + x_{2d} - \dot{x}_{1d} = -k_1 e_1 + e_2 \tag{15}$$

Consider the following Lyapunov function candidate:

$$V_1 = \frac{1}{2} {e_1}^2 \tag{16}$$

The time derivative of V_1 is

$$\dot{V}_1 = -k_1 {e_1}^2 + e_1 e_2 \tag{17}$$

If $e_2 = 0$, then $\dot{V}_1 \leq 0$.

Step 2 Taking the time derivative of $e_2 = x_2 - x_{2d}$, then

$$\dot{e}_2 = \dot{x}_2 - \dot{x}_{2d} = x_3 + g - \dot{x}_{2d} \tag{18}$$

Define $e_3 = x_3 - x_{3d}$ and a virtual controller x_{3d}.

$$x_{3d} = -\hat{g} + \dot{x}_{2d} - k_2 e_2 - e_1 \tag{19}$$

where k_2 is a positive constant and $\hat{g}$ is the estimated value of g.

From (14), the time derivative of x_{2d} is:

$$\dot{x}_{2d} = \ddot{x}_{1d} - k_1 \dot{e}_1 = \ddot{x}_{1d} - k_1 (x_2 - \dot{x}_{1d}) \tag{20}$$

From (18) and (19), the derivative of e_2 can be obtained as

$$\dot{e}_2 = e_3 + x_{3d} - \dot{x}_{2d} + g = g - \hat{g} - k_2 e_2 + e_3 - e_1 \tag{21}$$

Consider the following Lyapunov function candidate:

$$V_2 = V_1 + \frac{1}{2} {e_2}^2 \tag{22}$$

The time derivative of V_2 can be obtained as

$$\dot{V}_2 = -k_1 {e_1}^2 - k_2 {e_2}^2 + (g - \hat{g}) e_2 + e_2 e_3 \tag{23}$$

If $e_3 = 0$ and $\hat{g} = g$, then $\dot{V}_2 \leq 0$.

Step 3 Taking the time derivative of $e_3 = x_3 - x_{3d}$, then

$$\dot{e}_3 = \dot{x}_3 - \dot{x}_{3d} = x_4 - \dot{x}_{3d} \tag{24}$$

From (18), (19), (20) and (22), the time derivative of x_{3d} is:

$$\begin{aligned} \dot{x}_{3d} =& - \dot{\hat{g}} + \ddot{x}_{2d} - k_2 \dot{e}_2 - \dot{e}_1 \\ =& - \dot{\hat{g}} + \dddot{x}_{1d} - k_1 (x_3 + g - \ddot{x}_{1d}) \\ & - k_2 (x_3 + g - \dot{x}_{2d}) - x_2 + \dot{x}_{1d} \end{aligned} \tag{25}$$

We divide $\dot{x}_{3d}$ into two parts. $\dot{x}'_{3d}$ is the known part without model information, and $\bar{\dot{x}}_{3d}$ is the unknown part with model information (25), which can be rewritten as

$$\dot{x}_{3d} = \dot{x}'_{3d} - \bar{\dot{x}}_{3d} \tag{26}$$

where

$$\dot{x}'_{3d} = \dddot{x}_{1d} - k_1 (x_3 - \ddot{x}_{1d}) - k_2 (x_3 - \dot{x}_{2d}) - x_2 + \dot{x}_{1d} \tag{27}$$

$$\bar{\dot{x}}_{3d} = \dot{\hat{g}} + k_1 g + k_2 g \tag{28}$$

Define $e_4 = x_4 - x_{4d}$, $\bar{\dot{x}}_{3d} = d$ and a virtual controller x_{4d}. Choose a positive constant k_3, we have

$$x_{4d} = \dot{x}'_{3d} - \hat{d} - k_3 e_3 - e_2 \tag{29}$$

Substituting (26)–(29) into (24), we can get

$$\begin{aligned} \dot{e}_3 =& x_4 - \dot{x}_{3d} = x_4 - \dot{x}'_{3d} + \bar{\dot{x}}_{3d} \\ =& - k_3 e_3 - e_2 + e_4 + (d - \hat{d}) \end{aligned} \tag{30}$$

Consider the following Lyapunov function candidate:

$$V_3 = V_2 + \frac{1}{2}{e_3}^2 \tag{31}$$

The time derivative of V_3 can be obtained as

$$\begin{aligned}\dot{V}_3 =& -k_1{e_1}^2 - k_2{e_2}^2 - k_3{e_3}^2 + (g-\hat{g})e_2 \\ &+ (d-\hat{d})e_3 + e_3e_4\end{aligned} \tag{32}$$

If $e_4 = 0$, $\hat{g} = g$ and $\hat{d} = d$, then $\dot{V}_3 \leq 0$.

Step 4 To realize stability of control system, we take an actual controller into this step. The time derivative of $e_4 = x_4 - x_{4d}$ is

$$\dot{e}_4 = \dot{x}_4 - \dot{x}_{4d} = f + mu - \dot{x}_{4d} \tag{33}$$

From (24), (26), (27) and (29), the time derivative of x_{4d} is:

$$\begin{aligned}\dot{x}_{4d} =& -\dot{\hat{d}} + \ddot{x}'_{3d} - k_3\dot{e}_3 - \dot{e}_2 \\ =& \dddot{x}_{1d} - k_1(x_4 - \ddot{x}_{1d}) - k_2(x_4 - \dddot{x}_{1d} \\ &+ k_1(x_3 - \ddot{x}_{1d})) + \ddot{x}_{1d} - x_3 - k_3(x_4 - \dot{x}'_{3d}) \\ &- (x_3 - \dot{x}_{2d}) - k_1k_2g \\ &- g - \dot{\hat{d}} - k_3\bar{\dot{x}}_{3d} - g\end{aligned} \tag{34}$$

We divide $\dot{x}_{4d}$ into two parts. $\dot{x}'_{4d}$ is the known part without model information, and $\bar{\dot{x}}_{4d}$ is the unknown part with model information (34), which can be rewritten as

$$\dot{x}_{4d} = \dot{x}'_{4d} + \bar{\dot{x}}_{4d} \tag{35}$$

where

$$\begin{aligned}\dot{x}'_{4d} =& \dddot{x}_{1d} - k_2(x_4 - \ddot{x}_{1d} \\ &+ k_1(x_3 - \ddot{x}_{1d})) + \ddot{x}_{1d} - x_3 - k_3(x_4 - \dot{x}'_{3d}) \\ &- (x_3 - \dot{x}_{2d}) - k_1(x_4 - \ddot{x}_{1d})\end{aligned} \tag{36}$$

$$\bar{\dot{x}}_{4d} = -k_1k_2g - g - \dot{\hat{d}} - k_3\bar{\dot{x}}_{3d} - g \tag{37}$$

Define $h = f - \bar{\dot{x}}_{4d}$, and (33) can be rewritten as

$$\begin{aligned}\dot{e}_4 =& h + \bar{\dot{x}}_{4d} + mu - \dot{x}_{4d} \\ =& h - \dot{x}'_{4d} + (m-\hat{m})u + \hat{m}u\end{aligned} \tag{38}$$

where $\hat{m}$ is the estimated value of m.

Choosing the following control law

$$u = \frac{1}{\hat{m}}(-\hat{h} + \dot{x}'_{4d} - k_4e_4 - e_3) \tag{39}$$

where $\hat{h}$ is the estimated value of h and k_4 is a positive constant.

Substituting (39) into (38), we can get

$$\dot{e}_4 = (h - \hat{h}) - (m - \hat{m})u - k_4e_4 - e_3 \tag{40}$$

Consider the following Lyapunov function candidate:

$$V_4 = V_3 + \frac{1}{2}{e_4}^2 \tag{41}$$

The time derivative of V_4 can be obtained as

$$\begin{aligned}\dot{V}_4 =& -k_1{e_1}^2 - k_2{e_2}^2 - k_3{e_3}^2 \\ &- k_4{e_4}^2 + (m-\hat{m})ue_4 \\ &+ (g-\hat{g})e_2 + (d-\hat{d})e_3 + (h-\hat{h})e_4\end{aligned} \tag{42}$$

If $\hat{m} = m$, $\hat{g} = g$, $\hat{d} = d$ and $\hat{h} = h$, then $\dot{V}_4 \leq 0$.

4.2 Adaptive fuzzy controller

We use the proposed approximator in this section to approximate unknown nonlinear functions $g(x)$, $d(x)$ and $h(x)$, where the approximations are $\hat{g}(x)$, $\hat{h}(x)$ and $\hat{d}(x)$.

Taking the proposed adaptive factor into $g(x)$, $d(x)$ and $h(x)$, we can get

$$\begin{aligned}g(x) =& (1-\alpha_g)\underline{\xi}_g(x)\underline{\theta}_g^{*T} + \alpha_g\overline{\xi}_g(x)\overline{\theta}_g^{*T} \\ &+ (1-\alpha_g)\underline{\varepsilon}_g(x) + \alpha_g\overline{\varepsilon}_g(x)\end{aligned} \tag{43}$$

$$\begin{aligned}d(x) =& (1-\alpha_d)\underline{\xi}_d(x)\underline{\theta}_d^{*T} + \alpha_d\overline{\xi}_d(x)\overline{\theta}_d^{*T} \\ &+ (1-\alpha_d)\underline{\varepsilon}_d(x) + \alpha_d\overline{\varepsilon}_d(x)\end{aligned} \tag{44}$$

$$\begin{aligned}h(x) =& (1-\alpha_h)\underline{\xi}_h(x)\underline{\theta}_h^{*T} + \alpha_h\overline{\xi}_h(x)\overline{\theta}_h^{*T} \\ &+ (1-\alpha_h)\underline{\varepsilon}_h(x) + \alpha_h\overline{\varepsilon}_h(x)\end{aligned} \tag{45}$$

where $\underline{\varepsilon}_g(x)$ and $\overline{\varepsilon}_g(x)$, $\underline{\varepsilon}_d(x)$ and $\overline{\varepsilon}_d(x)$, $\underline{\varepsilon}_h(x)$ and $\overline{\varepsilon}_h(x)$ are the approximation errors; $\underline{\xi}_g$ and $\overline{\xi}_g$, $\underline{\xi}_d$ and $\overline{\xi}_d$, $\underline{\xi}_h$ and $\overline{\xi}_h$, are, respectively, the lower and the upper

membership functions; $\underline{\theta}_g^{*T}$ and $\overline{\theta}_g^{*T}$, $\underline{\theta}_d^{*T}$ and $\overline{\theta}_d^{*T}$, $\underline{\theta}_h^{*T}$ and $\overline{\theta}_h^{*T}$ are the optimal lower and upper approximation parameters of $g(x)$, $d(x)$ and $h(x)$. α_g, α_d, α_h are the adaptive factor.

According to the proposed approximator, the nonlinear functions $\hat{g}(x, \hat{\underline{\theta}}_g, \hat{\overline{\theta}}_g)$, $\hat{d}(x, \hat{\underline{\theta}}_d, \hat{\overline{\theta}}_d)$, $\hat{h}(x, \hat{\underline{\theta}}_h, \hat{\overline{\theta}}_h)$ can be expressed as

$$\hat{g}(x, \hat{\underline{\theta}}_g, \hat{\overline{\theta}}_g) = (1 - \hat{\alpha_g})\underline{\xi}_g(x)\hat{\underline{\theta}}_g^T + \hat{\alpha_g}\overline{\xi}_g(x)\hat{\overline{\theta}}_g^T \quad (46)$$

$$\hat{d}(x, \hat{\underline{\theta}}_d, \hat{\overline{\theta}}_d) = (1 - \hat{\alpha_d})\underline{\xi}_d(x)\hat{\underline{\theta}}_d^T + \hat{\alpha_d}\overline{\xi}_d(x)\hat{\overline{\theta}}_d^T \quad (47)$$

$$\hat{h}(x, \hat{\underline{\theta}}_h, \hat{\overline{\theta}}_h) = (1 - \hat{\alpha_h})\underline{\xi}_h(x)\hat{\underline{\theta}}_h^T + \hat{\alpha_h}\overline{\xi}_h(x)\hat{\overline{\theta}}_h^T \quad (48)$$

From (43) to (48), we have

$$\begin{aligned}
\tilde{g}(x) &= g(x) - \hat{g}(x, \hat{\underline{\theta}}_g, \hat{\overline{\theta}}_g) \\
&= (1 - \hat{\alpha}_g)\underline{\xi}_g(x)\tilde{\underline{\theta}}_g^T + \hat{\alpha}_g\overline{\xi}_g(x)\tilde{\overline{\theta}}_g^T \\
&\quad + (\overline{\xi}_g(x)\hat{\overline{\theta}}_g^T - \underline{\xi}_g(x)\hat{\underline{\theta}}_g^T)\tilde{\alpha}_g \\
&\quad + (\overline{\xi}_g(x)\tilde{\overline{\theta}}_g^T - \underline{\xi}_g(x)\tilde{\underline{\theta}}_g^T)\tilde{\alpha}_g \\
&\quad + (1 - \alpha_g)\underline{\varepsilon}_g(x) + \alpha_g\overline{\varepsilon}_g(x) \qquad (49) \\
\tilde{d}(x) &= d(x) - \hat{d}(x, \hat{\underline{\theta}}_d, \hat{\overline{\theta}}_d) \\
&= (1 - \hat{\alpha}_d)\underline{\xi}_d(x)\tilde{\underline{\theta}}_d^T + \hat{\alpha}_d\overline{\xi}_d(x)\tilde{\overline{\theta}}_d^T \\
&\quad + \left(\overline{\xi}_d(x)\hat{\overline{\theta}}_d^T - \underline{\xi}_d(x)\hat{\underline{\theta}}_d^T\right)\tilde{\alpha}_d \\
&\quad + \left(\overline{\xi}_d(x)\tilde{\overline{\theta}}_d^T - \underline{\xi}_d(x)\tilde{\underline{\theta}}_d^T\right)\tilde{\alpha}_d \\
&\quad + (1 - \alpha_d)\underline{\varepsilon}_d(x) + \alpha_d\overline{\varepsilon}_d(x) \qquad (50) \\
\tilde{h}(x) &= h(x) - \hat{h}(x, \hat{\underline{\theta}}_h, \hat{\overline{\theta}}_h) \\
&= (1 - \hat{\alpha}_h)\underline{\xi}_h(x)\tilde{\underline{\theta}}_h^T + \hat{\alpha}_h\overline{\xi}_h(x)\tilde{\overline{\theta}}_h^T \\
&\quad + \left(\overline{\xi}_h(x)\hat{\overline{\theta}}_h^T - \underline{\xi}_h(x)\hat{\underline{\theta}}_h^T\right)\tilde{\alpha}_h \\
&\quad + \left(\overline{\xi}_h(x)\tilde{\overline{\theta}}_h^T - \underline{\xi}_h(x)\tilde{\underline{\theta}}_h^T\right)\tilde{\alpha}_h \\
&\quad + (1 - \alpha_h)\underline{\varepsilon}_h(x) + \alpha_h\overline{\varepsilon}_h(x) \qquad (51)
\end{aligned}$$

where $\tilde{\underline{\theta}}_g = \underline{\theta}_g^* - \hat{\underline{\theta}}_g$, $\tilde{\overline{\theta}}_g = \overline{\theta}_g^* - \hat{\overline{\theta}}_g$, $\tilde{\underline{\theta}}_d = \underline{\theta}_d^* - \hat{\underline{\theta}}_d$, $\tilde{\overline{\theta}}_d = \overline{\theta}_d^* - \hat{\overline{\theta}}_d$, $\tilde{\underline{\theta}}_h = \underline{\theta}_h^* - \hat{\underline{\theta}}_h$, $\tilde{\overline{\theta}}_h = \overline{\theta}_h^* - \hat{\overline{\theta}}_h$, $\tilde{\alpha}_g = \alpha_g - \hat{\alpha}_g$, $\tilde{\alpha}_d = \alpha_d - \hat{\alpha}_d$ and $\tilde{\alpha}_h = \alpha_h - \hat{\alpha}_h$.

The adaptive law of m is chosen as nonlinear functions, which can be expressed as

$$\dot{\hat{m}} = \begin{cases} \gamma_m e_4 u, & e_4 u > 0 \\ \gamma_m e_4 u, & e_4 u \le 0, \hat{m} > \underline{m} \\ \gamma_m, & e_4 u \le 0, \hat{m} \le \underline{m} \end{cases} \quad (52)$$

where the initial value $\hat{m}(0) \ge \underline{m}$. If the estimated value of $\hat{m}$ is too small, then the control signal u will be too large. Thus $\hat{m}$ has a wide range of changes resulting in $\hat{m} = 0$. In order to prevent this situation, we choose the initial value $\hat{m}(0) = 500$, and then $\hat{m}$ can always be a large value.

The adaptive law of adaptive parameters are derived from Lyapunov stability analysis and chosen as

$$\dot{\hat{\theta}}_g = \begin{cases} \dot{\hat{\overline{\theta}}}_g = \overline{\gamma}_g e_2 \hat{\alpha}_g \overline{\xi}_g(x) - 2\overline{\lambda}_g \hat{\overline{\theta}}_g \\ \dot{\hat{\underline{\theta}}}_g = \underline{\gamma}_g e_2 (1 - \hat{\alpha}_g)\underline{\xi}_g(x) - 2\underline{\lambda}_g \hat{\underline{\theta}}_g \end{cases} \quad (53)$$

$$\dot{\hat{\theta}}_d = \begin{cases} \dot{\hat{\overline{\theta}}}_d = \overline{\gamma}_d e_3 \hat{\alpha}_d \overline{\xi}_d(x) - 2\overline{\lambda}_d \hat{\overline{\theta}}_d \\ \dot{\hat{\underline{\theta}}}_d = \underline{\gamma}_d e_3 (1 - \hat{\alpha}_d)\underline{\xi}_d(x) - 2\underline{\lambda}_d \hat{\underline{\theta}}_d \end{cases} \quad (54)$$

$$\dot{\hat{\theta}}_h = \begin{cases} \dot{\hat{\overline{\theta}}}_h = \overline{\gamma}_h e_4 \hat{\alpha}_h \overline{\xi}_h(x) - 2\overline{\lambda}_h \hat{\overline{\theta}}_h \\ \dot{\hat{\underline{\theta}}}_h = \underline{\gamma}_h e_4 (1 - \hat{\alpha}_d)\underline{\xi}_h(x) - 2\underline{\lambda}_h \hat{\underline{\theta}}_h \end{cases} \quad (55)$$

$$\dot{\hat{\alpha}}_g = \gamma_{\alpha_g} e_2 \left(\overline{\xi}_g(x)\hat{\overline{\theta}}_g^T - \underline{\xi}_g(x)\hat{\underline{\theta}}_g^T\right) - 2\lambda_{\alpha_g}\hat{\alpha}_g \quad (56)$$

$$\dot{\hat{\alpha}}_d = \gamma_{\alpha_d} e_3 \left(\overline{\xi}_d(x)\hat{\overline{\theta}}_d^T - \underline{\xi}_d(x)\hat{\underline{\theta}}_d^T\right) - 2\lambda_{\alpha_d}\hat{\alpha}_d \quad (57)$$

$$\dot{\hat{\alpha}}_h = \gamma_{\alpha_h} e_4 \left(\overline{\xi}_h(x)\hat{\overline{\theta}}_h^T - \underline{\xi}_h(x)\hat{\underline{\theta}}_h^T\right) - 2\lambda_{\alpha_h}\hat{\alpha}_h \quad (58)$$

where $\gamma = [\underline{\gamma}_g, \overline{\gamma}_g, \underline{\gamma}_d, \overline{\gamma}_d, \underline{\gamma}_h, \overline{\gamma}_h, \gamma_{\alpha_g}, \gamma_{\alpha_d}, \gamma_{\alpha_h}, \gamma_m]$ is the positive adaptation gain.

At the present stage, we summarize our main result in the following theorem, which shows that the designed controller guarantees the boundedness and stability of closed-loop system.

Theorem 1 *Consider a flexible-joint manipulator system as shown in (3), the control input u in (39) with the IT2FNN-based adaptive laws given by (52)–(58) guarantees that all the signals in the resulting closed-loop systems are bounded. Furthermore, given an attenuation factor ρ, the tracking performance of system will be satisfied*

$$\sum_{i=1}^{4}\int_0^T e_i^2(s)\mathrm{d}s \le \frac{1}{a_0}(V(0)+Tb_0 + \sum_{i=2}^{4}\int_0^T \rho^2 J_i^2 \mathrm{d}t, \quad T\in[0,\infty] \tag{59}$$

Proof of Theorem 1 To make the proof of stability more simple and clear, we define $m(x)$, $g(x)$, $d(x)$, $h(x)$ as $f_1(x)$, $f_2(x)$, $f_3(x)$, $f_4(x)$. Obviously, the approximation of $m(x)$, $g(x)$, $d(x)$, $h(x)$ is, respectively, $\hat{f}_1(x)$, $\hat{f}_2(x)$, $\hat{f}_3(x)$, $\hat{f}_4(x)$.

Consider the Lyapunov function candidate as

$$V = \frac{1}{2}\sum_{i=1}^{4} e_i^2 + \frac{1}{2\gamma_{f_1}}\tilde{f}_1^T\tilde{f}_1 + \sum_{i=2}^{4}\frac{1}{2\underline{\gamma}_{f_i}}\tilde{\underline{\theta}}_{f_i}^T\tilde{\underline{\theta}}_{f_i} + \sum_{i=2}^{4}\frac{1}{2\overline{\gamma}_{f_i}}\tilde{\overline{\theta}}_{f_i}^T\tilde{\overline{\theta}}_{f_i} + \sum_{i=2}^{4}\frac{1}{2\gamma_{\alpha_{f_i}}}\tilde{\alpha}_{f_i}^T\tilde{\alpha}_{f_i} \tag{60}$$

The time derivative of V is

$$\begin{aligned}\dot{V} =& -\sum_{i=1}^{4}k_i{e_i}^2 + \sum_{i=2}^{4}(f_i-\hat{f}_i)e_i - \sum_{i=2}^{4}\frac{1}{\underline{\gamma}_{f_i}}\tilde{\underline{\theta}}_{f_i}^T\dot{\underline{\hat{\theta}}}_{f_i} \\ &- \sum_{i=2}^{4}\frac{1}{\overline{\gamma}_{f_i}}\tilde{\overline{\theta}}_{f_i}^T\dot{\overline{\hat{\theta}}}_{f_i} - \sum_{i=2}^{4}\frac{1}{\gamma_{\alpha_{f_i}}}\tilde{\alpha}_{f_i}^T\dot{\hat{\alpha}}_{f_i} \\ &+ (f_1-\hat{f}_1)ue_4 - \frac{1}{\gamma_{f_1}}\tilde{f}_1^T\dot{\hat{f}}_1\end{aligned} \tag{61}$$

Applying (52), we get

$$\begin{aligned}\dot{V} \le& -\sum_{i=1}^{4}k_i{e_i}^2 + \sum_{i=2}^{4}(f_i-\hat{f}_i)e_i - \sum_{i=2}^{4}\frac{1}{\underline{\gamma}_{f_i}}\tilde{\underline{\theta}}_{f_i}^T\dot{\underline{\hat{\theta}}}_{f_i} \\ &- \sum_{i=2}^{4}\frac{1}{\overline{\gamma}_{f_i}}\tilde{\overline{\theta}}_{f_i}^T\dot{\overline{\hat{\theta}}}_{f_i} - \sum_{i=2}^{4}\frac{1}{\gamma_{\alpha_{f_i}}}\tilde{\alpha}_{f_i}^T\dot{\hat{\alpha}}_{f_i}\end{aligned} \tag{62}$$

Applying (49)–(51), $\dot{V}$ can be rewritten as

$$\begin{aligned}\dot{V} \le& -\sum_{i=1}^{4}k_i{e_i}^2 + \sum_{i=1}^{4}e_i\Big[(1-\hat{\alpha}_{f_i})\underline{\xi}_{f_i}(x)\tilde{\underline{\theta}}_{f_i}^T \\ &+ \hat{\alpha}_{f_i}\overline{\xi}_{f_i}(x)\tilde{\overline{\theta}}_{f_i}^T + \left(\overline{\xi}_{f_i}(x)\hat{\overline{\theta}}_{f_i}^T - \underline{\xi}_{f_i}(x)\hat{\underline{\theta}}_{f_i}^T\right)\tilde{\alpha}_{f_i}\Big] \\ &- \sum_{i=2}^{4}\frac{1}{\underline{\gamma}_{f_i}}\tilde{\underline{\theta}}_{f_i}^T\dot{\underline{\hat{\theta}}}_{f_i} - \sum_{i=2}^{4}\frac{1}{\overline{\gamma}_{f_i}}\tilde{\overline{\theta}}_{f_i}^T\dot{\overline{\hat{\theta}}}_{f_i} \\ &- \sum_{i=2}^{4}\frac{1}{\gamma_{\alpha_{f_i}}}\tilde{\alpha}_{f_i}^T\dot{\hat{\alpha}}_{f_i} + \sum_{i=2}^{4}e_i\Big[(1-\alpha_{f_i})\underline{\varepsilon}_{f_i}(x) \\ &+ \alpha_{f_i}\overline{\varepsilon}_{f_i}(x) + \left(\overline{\xi}_{f_i}(x)\tilde{\overline{\theta}}_{f_i}^T - \underline{\xi}_{f_i}(x)\tilde{\underline{\theta}}_{f_i}^T\right)\tilde{\alpha}_{f_i}\Big] \\ \le& -\sum_{i=1}^{4}k_i{e_i}^2 + \sum_{i=1}^{4}\tilde{\underline{\theta}}_{f_i}^T\Big[e_i(1-\hat{\alpha}_{f_i})\underline{\xi}_{f_i}(x) \\ &- \frac{1}{\underline{\gamma}_{f_i}}\dot{\underline{\hat{\theta}}}_{f_i}\Big] + \sum_{i=1}^{4}\tilde{\overline{\theta}}_{f_i}^T\left(e_i\hat{\alpha}_{f_i}\overline{\xi}_{f_i}(x) - \frac{1}{\overline{\gamma}_{f_i}}\dot{\overline{\hat{\theta}}}_{f_i}\right) \\ &+ \sum_{i=2}^{4}\tilde{\alpha}_{f_i}^T\Big[e_i(\overline{\xi}_{f_i}(x)\hat{\overline{\theta}}_{f_i}^T - \underline{\xi}_{f_i}(x)\hat{\underline{\theta}}_{f_i}^T) - \frac{1}{\gamma_{\alpha_{f_i}}}\dot{\hat{\alpha}}_{f_i}\Big] \\ &+ \sum_{i=2}^{4}e_i\Big[(1-\alpha_{f_i})\underline{\varepsilon}_{f_i}(x) + \alpha_{f_i}\overline{\varepsilon}_{f_i}(x) \\ &+ (\overline{\xi}_{f_i}(x)\tilde{\overline{\theta}}_{f_i}^T - \underline{\xi}_{f_i}(x)\tilde{\underline{\theta}}_{f_i}^T)\tilde{\alpha}_{f_i}\Big]\end{aligned} \tag{63}$$

We define $J_i = (1-\alpha_{f_i})\underline{\varepsilon}_{f_i}(x) + \alpha_{f_i}\overline{\varepsilon}_{f_i}(x) + (\overline{\xi}_{f_i}(x)\tilde{\overline{\theta}}_{f_i}^T - \underline{\xi}_{f_i}(x)\tilde{\underline{\theta}}_{f_i}^T)\tilde{\alpha}_{f_i}$, $i=2,3,4$, and applying (53)–(58) into the time derivative of the Lyapunov function $\dot{V}$, we have

$$\begin{aligned}\dot{V} \le& -\sum_{i=1}^{4}k_i{e_i}^2 + \sum_{i=2}^{4}\frac{2\underline{\lambda}_{f_i}}{\underline{\gamma}_{f_i}}\tilde{\underline{\theta}}_{f_i}^T\hat{\underline{\theta}}_{f_i} + \sum_{i=2}^{4}\frac{2\overline{\lambda}_{f_i}}{\overline{\gamma}_{f_i}}\tilde{\overline{\theta}}_{f_i}^T\hat{\overline{\theta}}_{f_i} \\ &+ \sum_{i=2}^{4}\frac{2\lambda_{\alpha_{f_i}}}{\gamma_{\alpha_{f_i}}}\tilde{\alpha}_{f_i}^T\hat{\alpha_{f_i}} + \sum_{i=2}^{4}e_iJ_i\end{aligned} \tag{64}$$

Setting $c_i = k_i - \frac{1}{2\rho^2}$, we have

$$\begin{aligned}\dot{V} \le& -\sum_{i=1}^{4}c_i{e_i}^2 - \sum_{i=1}^{4}\frac{1}{2\rho^2}{e_i}^2 + \sum_{i=2}^{4}\frac{2\underline{\lambda}_{f_i}}{\underline{\gamma}_{f_i}}\tilde{\underline{\theta}}_{f_i}^T\hat{\underline{\theta}}_{f_i} \\ &+ \sum_{i=2}^{4}\frac{2\overline{\lambda}_{f_i}}{\overline{\gamma}_{f_i}}\tilde{\overline{\theta}}_{f_i}^T\hat{\overline{\theta}}_{f_i} + \sum_{i=2}^{4}\frac{2\lambda_{\alpha_{f_i}}}{\gamma_{\alpha_{f_i}}}\tilde{\alpha}_{f_i}^T\hat{\alpha}_{f_i} + \sum_{i=2}^{4}e_iJ_i\end{aligned} \tag{65}$$

Since $-\frac{1}{2a^2}b^2 + bc \le \frac{1}{2}a^2c^2$, we have

$$\begin{aligned}\dot{V} \le & -\sum_{i=1}^{4} c_i {e_i}^2 - \frac{1}{2\rho^2}{e_1}^2 + \sum_{i=2}^{4}\rho^2 J_i^2 \\ & + \sum_{i=2}^{4}\frac{2\overline{\lambda}_{f_i}}{\overline{\gamma}_{f_i}}\tilde{\overline{\theta}}_{f_i}^T\hat{\overline{\theta}}_{f_i} + \sum_{i=2}^{4}\frac{2\lambda_{\alpha_{f_i}}}{\gamma_{\alpha_{f_i}}}\tilde{\alpha}_{f_i}^T\hat{\alpha}_{f_i} \\ & + \sum_{i=2}^{4}\frac{2\underline{\lambda}_{f_i}}{\underline{\gamma}_{f_i}}\tilde{\underline{\theta}}_{f_i}^T\hat{\underline{\theta}}_{f_i} \\ \le & -\sum_{i=1}^{4} c_i {e_i}^2 - \frac{1}{2\rho^2}{e_1}^2 + \sum_{i=2}^{4}\rho^2 J_i^2 \\ & + \sum_{i=2}^{4}\frac{\underline{\lambda}_{f_i}}{\underline{\gamma}_{f_i}}\left(2{\underline{\theta}_{f_i}^*}^T\hat{\underline{\theta}}_{f_i} - 2\hat{\underline{\theta}}_{f_i}^T\hat{\underline{\theta}}_{f_i}\right) \\ & + \sum_{i=2}^{4}\frac{\overline{\lambda}_{f_i}}{\overline{\gamma}_{f_i}}\left(2{\overline{\theta}_{f_i}^*}^T\hat{\overline{\theta}}_{f_i} - 2\hat{\overline{\theta}}_{f_i}^T\hat{\overline{\theta}}_{f_i}\right) \\ & + \sum_{i=2}^{4}\frac{\lambda_{\alpha_{f_i}}}{\gamma_{\alpha_{f_i}}}\left(2{\alpha_{f_i}^*}^T\hat{\alpha}_{f_i} - 2\hat{\alpha_{f_i}}^T\hat{\alpha}_{f_i}\right) \end{aligned} \tag{66}$$

Since ${a^*}^T a^* + \hat{a}^T\hat{a} \ge 2{a^*}^T\hat{a}$, and thus $2{a^*}^T\hat{a} - 2\hat{a}^T\hat{a} \le {a^*}^T a^* - \hat{a}^T\hat{a}$, we can get

$$\begin{aligned}\dot{V} \le & -\sum_{i=1}^{4} c_i {e_i}^2 - \frac{1}{2\rho^2}{e_1}^2 + \sum_{i=2}^{4}\rho^2 J_i^2 \\ & + \sum_{i=2}^{4}\frac{\underline{\lambda}_{f_i}}{\underline{\gamma}_{f_i}}\left({\underline{\theta}_{f_i}^*}^T\underline{\theta}_{f_i}^* - \hat{\underline{\theta}}_{f_i}^T\hat{\underline{\theta}}_{f_i}\right) \\ & + \sum_{i=2}^{4}\frac{\overline{\lambda}_{f_i}}{\overline{\gamma}_{f_i}}({\overline{\theta}_{f_i}^*}^T\overline{\theta}_{f_i}^* - \hat{\overline{\theta}}_{f_i}^T\hat{\overline{\theta}}_{f_i}) \\ & + \sum_{i=2}^{4}\frac{\lambda_{\alpha_{f_i}}}{\gamma_{\alpha_{f_i}}}\left({\alpha_{f_i}^*}^T\alpha_{f_i}^* - \hat{\alpha}_{f_i}^T\hat{\alpha}_{f_i}\right) \\ \le & -\sum_{i=1}^{4} c_i {e_i}^2 - \frac{1}{2\rho^2}{e_1}^2 + \sum_{i=2}^{4}\rho^2 J_i^2 \\ & + \sum_{i=2}^{4}\frac{\underline{\lambda}_{f_i}}{\underline{\gamma}_{f_i}}(-{\underline{\theta}_{f_i}^*}^T\underline{\theta}_{f_i}^* - \hat{\underline{\theta}}_{f_i}^T\hat{\underline{\theta}}_{f_i}) \\ & + \sum_{i=2}^{4}\frac{\overline{\lambda}_{f_i}}{\overline{\gamma}_{f_i}}\left(-{\overline{\theta}_{f_i}^*}^T\overline{\theta}_{f_i}^* - \hat{\overline{\theta}}_{f_i}^T\hat{\overline{\theta}}_{f_i}\right) \\ & + \sum_{i=2}^{4}\frac{\lambda_{\alpha_{f_i}}}{\gamma_{\alpha_{f_i}}}\left(-{\alpha_{f_i}^*}^T\alpha_{f_i}^* - \hat{\alpha}_{f_i}^T\hat{\alpha}_{f_i}\right) \\ & + \sum_{i=2}^{4}\frac{2\underline{\lambda}_{f_i}}{\underline{\gamma}_{f_i}}{\underline{\theta}_{f_i}^*}^T\underline{\theta}_{f_i}^* + \sum_{i=2}^{4}\frac{2\lambda_{\alpha_{f_i}}}{\gamma_{\alpha_{f_i}}}{\alpha_{f_i}^*}^T\alpha_{f_i}^* \\ & + \sum_{i=2}^{4}\frac{2\overline{\lambda}_{f_i}}{\overline{\gamma}_{f_i}}{\overline{\theta}_{f_i}^*}^T\overline{\theta}_{f_i}^* \end{aligned} \tag{67}$$

Since $\tilde{a}^T\tilde{a} = (a^*-\hat{a})^T(a^*-\hat{a}) = {a^*}^T a^* - 2{a^*}^T\hat{a} + \hat{a}^T\hat{a} \le 2{a^*}^T a^* + 2\hat{a}^T\hat{a}$, we have $-\frac{1}{2}\tilde{a}^T\tilde{a} \ge -\hat{a}^T\hat{a} - {a^*}^T a^*$. The time derivative of the Lyapunov function V can be obtained as follows

$$\begin{aligned}\dot{V} \le & -\sum_{i=1}^{4} c_i {e_i}^2 - \frac{1}{2\rho^2}{e_1}^2 + \sum_{i=2}^{4}\rho^2 J_i^2 \\ & - \sum_{i=2}^{4}\frac{\underline{\lambda}_{f_i}}{2\underline{\gamma}_{f_i}}\tilde{\underline{\theta}}_{f_i}^T\tilde{\underline{\theta}}_{f_i} - \sum_{i=2}^{4}\frac{\overline{\lambda}_{f_i}}{2\overline{\gamma}_{f_i}}\tilde{\overline{\theta}}_{f_i}^T\tilde{\overline{\theta}}_{f_i} \\ & - \sum_{i=2}^{4}\frac{\lambda_{\alpha_{f_i}}}{2\gamma_{\alpha_{f_i}}}\tilde{\alpha}_{f_i}^T\tilde{\alpha}_{f_i} + \sum_{i=2}^{4}\frac{2\underline{\lambda}_{f_i}}{\underline{\gamma}_{f_i}}{\underline{\theta}_{f_i}^*}^T\underline{\theta}_{f_i}^* \\ & + \sum_{i=2}^{4}\frac{2\lambda_{\alpha_{f_i}}}{\gamma_{\alpha_{f_i}}}{\alpha_{f_i}^*}^T\alpha_{f_i}^* + \sum_{i=2}^{4}\frac{2\overline{\lambda}_{f_i}}{\overline{\gamma}_{f_i}}{\overline{\theta}_{f_i}^*}^T\overline{\theta}_{f_i}^* \end{aligned} \tag{68}$$

To guarantee $k_i \ge \frac{1}{2\rho^2}$, we define $c_i, i = 1, \ldots, 4$ is a positive constant and $c_0 = \min\{\frac{2\rho^2 c_1 + 1}{\rho^2}, 2c_i, \underline{\lambda}_{f_i}, \overline{\lambda}_{f_i}, \lambda_{\alpha_{f_i}}; i = 2, 3, 4\}$. The time derivative of the Lyapunov function $\dot{V}$ can be rewritten as

$$\begin{aligned}\dot{V} \le & -c_0\left(\sum_{i=1}^{4}\frac{1}{2}e_i^2 + \frac{1}{2\gamma_{f_1}}\tilde{f}_1^T\tilde{f}_1 + \sum_{i=2}^{4}\frac{1}{2\underline{\gamma}_{f_i}}\tilde{\underline{\theta}}_{f_i}^T\tilde{\underline{\theta}}_{f_i}\right. \\ & \left. + \sum_{i=2}^{4}\frac{1}{2\overline{\gamma}_{f_i}}\tilde{\overline{\theta}}_{f_i}^T\tilde{\overline{\theta}}_{f_i} + \sum_{i=2}^{4}\frac{1}{2\gamma_{\alpha_{f_i}}}\tilde{\alpha}_{f_i}^T\tilde{\alpha}_{f_i}\right) \\ & + \sum_{i=2}^{4}\frac{2\underline{\lambda}_{f_i}}{\underline{\gamma}_{f_i}}{\underline{\theta}_{f_i}^*}^T\underline{\theta}_{f_i}^* + \sum_{i=2}^{4}\frac{2\overline{\lambda}_{f_i}}{\overline{\gamma}_{f_i}}{\overline{\theta}_{f_i}^*}^T\overline{\theta}_{f_i}^* \\ & + \sum_{i=2}^{4}\frac{2\lambda_{\alpha_{f_i}}}{\gamma_{\alpha_{f_i}}}{\alpha_{f_i}^*}^T\alpha_{f_i}^* + \frac{c_0}{2\gamma_{f_1}}\tilde{f}_1^T\tilde{f}_1 + \sum_{i=2}^{4}\rho^2 J_i^2 \end{aligned} \tag{69}$$

Define $c_{V\max} = \sum_{i=2}^{4} \frac{2\underline{\lambda}_{f_i}}{\underline{\gamma}_{f_i}} \underline{\theta}_{f_i}^{*T} \underline{\theta}_{f_i}^{*} + \sum_{i=2}^{4} \frac{2\overline{\lambda}_{f_i}}{\overline{\gamma}_{f_i}} \overline{\theta}_{f_i}^{*T} \overline{\theta}_{f_i}^{*} + \sum_{i=2}^{4} \frac{2\lambda_{\alpha_{f_i}}}{\gamma_{\alpha_{f_i}}} \alpha_{f_i}^{*T} \alpha_{f_i}^{*} + \frac{c_0}{2\gamma_{f_1}} \tilde{f}_1^T \tilde{f}_1 + \sum_{i=2}^{4} \rho^2 J_i^2$, we get

$$\dot{V} \le c_0 V + c_{V\max} \tag{70}$$

Integrating (70) over $[0, t]$, we have

$$\begin{aligned} V(t) &\le V(0)\exp(-c_0 t) + \frac{c_{V\max}}{c_0}(1 - \exp(-c_0 t)) \\ &\le V(0) + \frac{c_{V\max}}{c_0}, t \ge 0 \end{aligned} \tag{71}$$

We define the tight set $\Omega_0 = \{X | V(X) \le C_0\}$, where $C_0 = V(0) + \frac{c_{V\max}}{c_0}$. Then we can conclude that all the signals in the closed-loop system are bounded.

Setting $a_0 = \min\{c_1 + \frac{1}{2\rho^2}, c_i, i = 2, 3, 4\}$ and (68) can be rewritten as

$$\begin{aligned} \dot{V} \le & -a_0 \sum_{i=1}^{4} {e_i}^2 + \sum_{i=2}^{4} \rho^2 J_i^2 - \sum_{i=2}^{4} \frac{\underline{\lambda}_{f_i}}{2\underline{\gamma}_{f_i}} \tilde{\underline{\theta}}_{f_i}^T \tilde{\underline{\theta}}_{f_i} \\ & - \sum_{i=2}^{4} \frac{\overline{\lambda}_{f_i}}{2\overline{\gamma}_{f_i}} \tilde{\overline{\theta}}_{f_i}^T \tilde{\overline{\theta}}_{f_i} - \sum_{i=2}^{4} \frac{\lambda_{\alpha_{f_i}}}{2\gamma_{\alpha_{f_i}}} \tilde{\alpha}_{f_i}^T \tilde{\alpha}_{f_i} + b_0 \\ \le & -a_0 \sum_{i=1}^{4} {e_i}^2 + b_0 + \sum_{i=2}^{4} \rho^2 J_i^2 \end{aligned} \tag{72}$$

where $b_0 = \sum_{i=2}^{4} \frac{2\underline{\lambda}_{f_i}}{\underline{\gamma}_{f_i}} \underline{\theta}_{f_i}^{*T} \underline{\theta}_{f_i}^{*} + \sum_{i=2}^{4} \frac{2\lambda_{\alpha_{f_i}}}{\gamma_{\alpha_{f_i}}} \alpha_{f_i}^{*T} \alpha_{f_i}^{*} + \sum_{i=2}^{4} \frac{2\overline{\lambda}_{f_i}}{\overline{\gamma}_{f_i}} \overline{\theta}_{f_i}^{*T} \overline{\theta}_{f_i}^{*}$

Integrating (72) over $[0, t]$, we have

$$\begin{aligned} \int_0^T \dot{V} \mathrm{d}t \le & -\int_0^T a_0 \sum_{i=1}^{4} e_i^2(s)\mathrm{d}s + T b_0 \\ & + \sum_{i=2}^{4} \int_0^T \rho^2 J_i^2 \mathrm{d}t \end{aligned} \tag{73}$$

Since $\int_0^T \dot{V}\mathrm{d}t = V(T) - V(0)$, we have

$$\begin{aligned} \sum_{i=1}^{4} \int_0^T e_i^2(s)\mathrm{d}s \le & -\frac{1}{a_0}\Big(V(0) - V(T) + T b_0 \\ & + \sum_{i=2}^{4} \int_0^T \rho^2 J_i^2 \mathrm{d}t\Big) \end{aligned} \tag{74}$$

Since $-\frac{1}{a_0} V(T) \le 0$, we get

$$\begin{aligned} \sum_{i=1}^{4} \int_0^T e_i^2(s)\mathrm{d}s \le & \frac{1}{a_0}\Big(V(0) + T b_0 \\ & + \sum_{i=2}^{4} \int_0^T \rho^2 J_i^2 \mathrm{d}t\Big) \end{aligned} \tag{75}$$

That is, given an attenuation factor ρ, the accuracy of tracking error is determined by the upper bound of approximation error. Thus, the theorem is proved. □

5 Experimental results

In this section, we demonstrate the effectiveness of the proposed scheme on a single-link flexible-joint manipulator. The actual values of parameters for dynamic equations (3) are $M = 0.2\,\mathrm{kg}$, $L = 0.02\,\mathrm{m}$, $I = 1.35 \times 10^{-3}\,\mathrm{kg\,m^2}$, $K = 7.47N\,\mathrm{m/rad}$, $J = 2.16 \times 10^{-1}\,\mathrm{kg\,m^2}$. Three IT2FNN are used to approximate the nonlinear functions $g(x)$, $d(x)$ and $h(x)$. $x = [x_1, x_2, x_3, x_4]$ is the vector input. For each input x_i, type-2 Gaussian membership functions are chosen as

$$\hat{F}_i^j = \begin{cases} \mu_{\underline{F}_i^j}(x_i) = a\exp\left(-\frac{1}{2}\left(\frac{x_i + c_j}{\sigma_j}\right)\right) \\ \mu_{\overline{F}_i^j}(x_i) = \exp\left(-\frac{1}{2}\left(\frac{x_i + c_j}{\sigma_j}\right)\right) \end{cases} \tag{76}$$

where $i = 1, 2, 3, 4$, $j = 1, 2, 3$, $c = [c_1, c_2, c_3] = [1.25, 0, -1.25]$, $\sigma = [\sigma_1, \sigma_2, \sigma_3] = [0.6, 0.6, 0.6]$ and $a = 0.8$.

The other design parameters are chosen as: $\underline{m} = 1$, $\gamma = [\underline{\gamma}_g, \overline{\gamma}_g, \underline{\gamma}_d, \overline{\gamma}_d, \underline{\gamma}_h, \overline{\gamma}_h, \gamma_{\alpha_g}, \gamma_{\alpha_d}, \gamma_{\alpha_h}, \gamma_m] = [200, 500, 200, 500, 200, 500, 0.05, 0.05, 0.05, 0.006]$, $\lambda = [\underline{\lambda}_g, \overline{\lambda}_g, \underline{\lambda}_d, \overline{\lambda}_d, \underline{\lambda}_h, \overline{\lambda}_h, \lambda_{\alpha_g}, \lambda_{\alpha_d}, \lambda_{\alpha_h}] = [10, 10, 10, 10, 11.25, 11.25, 0.001, 0.001, 0.001]$.

The initial conditions are set as: $x(0) = [x_1(0), x_2(0), x_3(0), x_4(0)] = [0, 0, 0, 0]$, $\hat{\theta}_g(0) = [\underline{\hat{\theta}}_g(0), \overline{\hat{\theta}}_g(0)] = [1.2, 1.2]$, $\hat{\theta}_d(0) = [\underline{\hat{\theta}}_d(0), \overline{\hat{\theta}}_d(0)] = [1.2, 1.2]$, $\hat{\theta}_h(0) = [\underline{\hat{\theta}}_h(0), \overline{\hat{\theta}}_h(0)] = [1.2, 1.2]$, $\hat{\alpha}_g(0) = 0$, $\hat{\alpha}_d(0) = 0$, $\hat{\alpha}_h(0) = 0$, $\hat{m}(0) = 500$. The desired output trajectory is designed to be $y_d = 0.2\sin(t)$. The control target is that the system output can track the desired trajectory even in the case of external disturbance $d(t) = 0.05\cos(2t)$.

To evaluate the performance of all controllers with difference approximator (T1FNN, NN, IT2FNN) clearly, we use the following performance criterions: the integral of square error (ISE), the integral of the absolute value of the error (IAE) and the integral of the time multiplied by the absolute value of the error (ITAE), which can be expressed as:

$$\begin{aligned} \text{ISE} &= \int_0^\infty [e(t)]^2 \mathrm{d}t \\ \text{IAE} &= \int_0^\infty |e(t)| \, \mathrm{d}t \\ \text{ITAE} &= \int_0^\infty t \, |e(t)| \, \mathrm{d}t \end{aligned} \tag{77}$$

Simulation results demonstrate the superior performance of the proposed controller. The responses of the system states q_1, $\dot{q}_1$, q_2, $\dot{q}_2$ are illustrated in Figs. 3 and 4. The trajectory of control input is shown in Fig. 5. It is clear that the control input is bounded. Tracking curves are depicted in Fig. 6. We can find that three approximators have the ability to achieve precise tracking. However, the accuracy of each approximator is different. Figure 7 demonstrates that the proposed controller has better steady-state performance, less fluctuation and higher approximation accuracy than T1FNN and NN. It is noted that the tracking error tends to a small neighborhood of zero even though there is external disturbance.

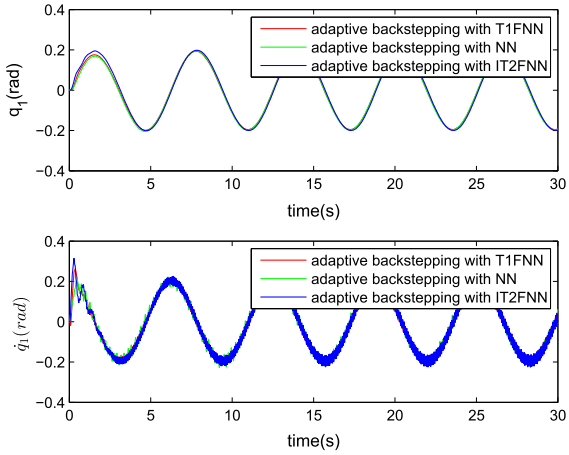

Fig. 3 Responses of q_1 and $\dot{q}_1$

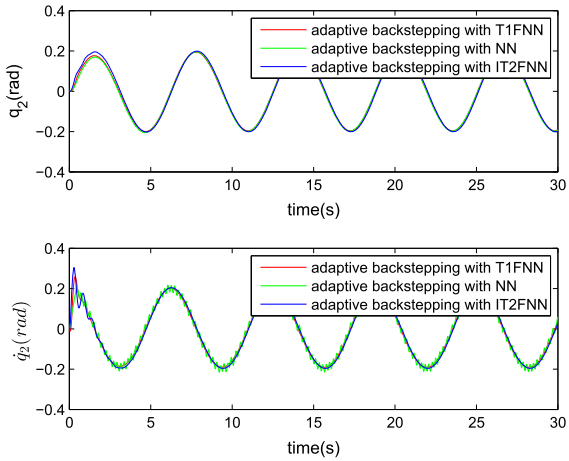

Fig. 4 Responses of q_2 and $\dot{q}_2$

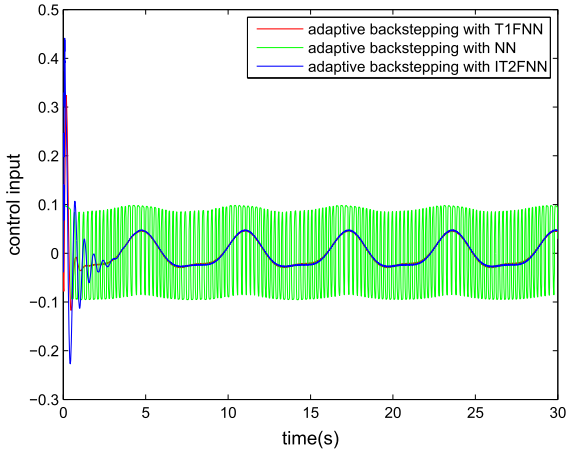

Fig. 5 Trajectories of control input

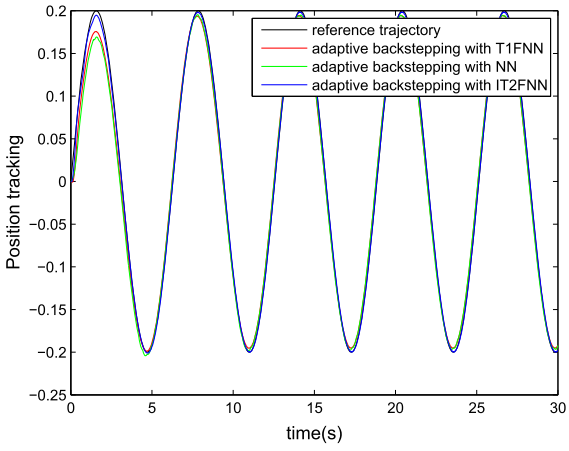

Fig. 6 Position tracking performance

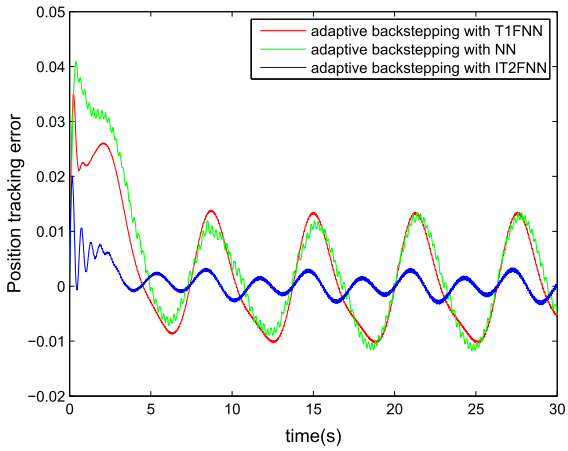

Fig. 7 Position tracking error

Table 1 Performance index

	T1FNN	NN	IT2FNN
ISE	0.0034	0.0047	0.0003
IAE	0.2555	0.2785	0.0615
ITAE	3.1988	3.2342	0.6950

Table 1 lists the ISE, IAE and ITAE for all controllers. The values of the ISE, the IAE and the ITAE for the proposed controller with the IT2FNN approximator are lower than those obtained for the T1FNN and the NN approximator. It is clear that the adaptive backstepping controller with the IT2FNN approximator is able to achieve better tracking performance and high accuracy.

Compared to the existing control method for flexible-joint manipulator in recent years [46], the adaptive backstepping controller with the IT2FNN approximator has the obvious advantages in transient tracking performance and high accuracy. From the results of simulation without external disturbance in [46], it can be seen that the maximum tracking error is about 0.25 rad and the tracking error tends to a small neighborhood of zero at about 3.75 s. In this study, the maximum tracking error is 0.02 rad and reduces to less than 0.005 rad at 2.57 s even though there is external disturbance. Starting from 3.08 s, the range of the tracking error is stable between 0.002 rad and $2.1e^{-5}$ rad. The time it takes for the tracking error to a small neighborhood of zero is about 0.31 times shorter than the control method in [46]. It can demonstrate that the proposed method significantly eliminates the undesirable overshoot and reduces the settling time. Therefore, the proposed adaptive backstepping controller with the IT2FNN approximator can obtain better steady-state performance and improve approximation accuracy.

6 Conclusions

In this paper, an adaptive backstepping control scheme based on IT2FNN approximator has been proposed for a flexible-joint manipulator with mismatched uncertainties. The IT2FNN is used to approximate the unknown functions. The stability analysis of the proposed scheme is derived. The proposed adaptive controller guarantees that all the signals in the resulting closed-loop systems are bounded. Finally, the simulation results of the comparative study illustrate that the performances of adaptive backstepping control based on IT2FNN approximator over the others.

Acknowledgements This work is supported by the National Natural Science Foundation of China (61703291) and the Applied Basic Research Program of Science and Technology Department of Sichuan Province, China (2016JY0085).

Compliance with ethical standards

Conflict of interest No potential conflict of interest was reported by the authors.

References

1. Khoygani, M.R.R., Ghasemi, R., Vali, A.R.: Intelligent nonlinear observer design for a class of nonlinear discrete-time flexible joint robot. Intell. Serv. Robot. **8**(1), 45–56 (2015)
2. Fateh, M.M.: Nonlinear control of electrical flexible-joint robots. Nonlinear Dyn. **67**(4), 2549–2559 (2012)
3. Yun, J.N., Su, J.B.: Design of a disturbance observer for a two-link manipulator with flexible joints. IEEE Trans. Control Syst. Technol. **22**(2), 809–815 (2014)
4. Singh, J.P., Lochan, K., Kuznetsov, N.V., et al.: Coexistence of single- and multi-scroll chaotic orbits in a single-link flexible joint robot manipulator with stable spiral and index-4 spiral repellor types of equilibria. Nonlinear Dyn. **90**(2), 1277–1299 (2017)
5. Bian, Y., Gao, Z., Yun, C.: Motion control of the flexible manipulator via controllable local degrees of freedom. Nonlinear Dyn. **55**(4), 373–384 (2009)
6. Izadbakhsh, A.: Robust control design for rigid-link flexible-joint electrically driven robot subjected to constraint: theory and experimental verification. Nonlinear Dyn. **85**(2), 751–765 (2016)

7. Kim, M.J., Park, Y.J., Chung, W.K.: Design of a momentum-based disturbance observer for rigid and flexible joint robots. Intell. Serv. Robot. **8**(1), 57–65 (2015)
8. Chalhoub, N.G., Kfoury, G.A.: Development of a robust nonlinear observer for a single-link flexible manipulator. Nonlinear Dyn. **39**(3), 217–233 (2005)
9. Luca, A.D., Albu-Schaffer, A., Haddadin, S., et al.: Collision detection and safe reaction with the DLR-III lightweight manipulator arm. In: IEEE/RSJ International Conference on Intelligent Robots & Systems (2007)
10. Zouari, L., Abid, H., Abid, M.: Sliding mode and PI controllers for uncertain flexible joint manipulator. Int. J. Autom. Comput. **12**(2), 117–124 (2015)
11. Spong, M.W., Khorasani, K., Kokotovic, P.V.: An integral manifold approach to the feedback control of flexible joint robots. IEEE J. Robot. Autom. **3**(4), 291–300 (1987)
12. Ghorbel, F., Hung, J.Y., Spong, M.W.: Adaptive control of flexible-joint manipulators. Control Syst. Mag. IEEE **9**(7), 9–13 (1989)
13. Oh, J.H., Lee, J.S.: Control of flexible joint robot system by backstepping design approach. Intell. Autom. Soft Comput. **5**(4), 12 (1999)
14. Kim, M.J., Chung, W.K.: Disturbance-observer-based pd control of flexible joint robots for asymptotic convergence. IEEE Trans. Robot. **31**(6), 1–9 (2015)
15. Kugi, A., Ott, C., Albu-Schaffer, A., et al.: On the passivity-based impedance control of flexible joint robots. IEEE Trans. Robot. **24**(2), 416–429 (2008)
16. Liu, Z.G., Huang, J.M.: A new adaptive tracking control approach for uncertain flexible joint robot system. Int. Autom. Comput. **12**(5), 559–566 (2015)
17. Huang, A.C., Chen, et al.: Adaptive sliding control for single-link flexible-joint robot with mismatched uncertainties. IEEE Trans. Control Syst. Technol. **12**(5), 770–775 (2004)
18. Liu, Y.J., Li, S., Tong, S., et al.: Adaptive reinforcement learning control based on neural approximation for nonlinear discrete-time systems with unknown nonaffine dead-zone input. IEEE Trans. Neural Netw. Learn. Syst. **99**, 1–11 (2018)
19. Zhao, T., Liu, J., Dian, S.: Finite-time control for interval type-2 fuzzy time-delay systems with norm-bounded uncertainties and limited communication capacity. Inf. Sci. **483**, 153–173 (2019)
20. Li, Y., Liu, L., Feng, G.: Robust adaptive output feedback control to a class of non-triangular stochastic nonlinear systems. Automatica **89**, 325–332 (2018)
21. Miao, Z., Wang, Y.: Robust dynamic surface control of flexible joint robots using recurrent neural networks. J. Control Theory Appl. **11**(2), 222–229 (2013)
22. Yoo, S.J., Park, J.B., Choi, Y.H.: Adaptive dynamic surface control of flexible-joint robots using self-recurrent wavelet neural networks. IEEE Trans. Syst. Man Cybern. Part B Cybern. A Publ. IEEE Syst. Man Cybern. Soc. **36**(6), 1342–55 (2006)
23. Macnab, C.J.B.: Improved output tracking of a flexible-joint arm using neural networks. Neural Process. Lett. **32**(2), 201–218 (2010)
24. He, W., Yan, Z., Sun, Y., et al.: Neural-learning-based control for a constrained robotic manipulator with flexible joints. In: IEEE Transactions on Neural Networks and Learning Systems, pp. 1–11 (2018)
25. Liu, J.K.: Design of Robot Control System and MATLAB Simulation. Tsinghua University Press, Beijing (2008)
26. Li, Y., Tong, S., Li, T.: Fuzzy adaptive dynamic surface control for a single-link flexible-joint robot. Nonlinear Dyn. **70**(3), 2035–2048 (2012)
27. Park, C.W., Cho, Y.W.: Adaptive tracking control of flexible joint manipulator based on fuzzy model reference approach. IEE Proc. Control Theory Appl. **150**(2), 198 (2003)
28. Liu, J., Zha, L., Xie, X., et al.: Resilient observer-based control for networked nonlinear TCS fuzzy systems with hybrid-triggered scheme. Nonlinear Dyn. **91**(3), 2049–2061 (2018)
29. Li, H., Gao, Y., Shi, P., et al.: Observer-based fault detection for nonlinear systems with sensor fault and limited communication capacity. IEEE Trans. Autom. Control **61**(9), 2745–2751 (2016)
30. Xie, X., Yue, D., Peng, C.: Multi-instant switching control of nonlinear networked systems under unreliable wireless digital channels. J. Frankl. Inst. **354**(9), 3872–3884 (2017)
31. Su, X., Xia, F., Liu, J., et al.: Event-triggered fuzzy control of nonlinear systems with its application to inverted pendulum systems. Automatica **94**, 236–248 (2018)
32. Zhou, H.B., Ying, H., Duan, J.A.: Adaptive control using interval type-2 fuzzy logic for uncertain nonlinear systems. J. Cent. S. Univ. Technol. **18**(3), 760–766 (2011)
33. Oh, S.K., Jang, H.J., Pedrycz, W.: A comparative experimental study of type-1/type-2 fuzzy cascade controller based on genetic algorithms and particle swarm optimization. Expert Syst. Appl. **38**(9), 11217–11229 (2011)
34. Xie, T.T., Yu, H., Wilamowski, B.M.: Comparison of Fuzzy and Neural Systems for Implementation of Nonlinear Control Surfaces// Human–Computer Systems Interaction: Backgrounds and Applications 2. Springer, Berlin (2012)
35. Zhao, T., Dian, S.: State feedback control for interval type-2 fuzzy systems with time-varying delay and unreliable communication links. IEEE Trans. Fuzzy Syst. **26**(2), 951–966 (2018)
36. Mohammadzadeh, A., Ghaemi, S., Kaynak, O., et al.: Observer-based method for synchronization of uncertain fractional order chaotic systems by the use of a general type-2 fuzzy system. Appl. Soft Comput. **49**, 544–560 (2016)
37. Li, Y.M., Yang, Y., Li, L.: Adaptive backstepping fuzzy control based on type-2 fuzzy system. J. Appl. Math. **2012**(3), 295–305 (2012)
38. Ezziani, N., Hussain, A., Essounbouli, N., et al.: Backstepping adaptive type-2 fuzzy controller for induction machine. In: IEEE International Symposium on Industrial Electronics, 2008. ISIE 2008. IEEE (2008)
39. Meskine, K., Khaber, F.: Robust backstepping control for uncertain chaotic multi-inputs multi-outputs systems using type 2 fuzzy systems. Trans. Inst. Meas. Control (2018). https://doi.org/10.1177/0142331217742965
40. Chaoui, H., Gueaieb, W.: Type-2 fuzzy logic control of a flexible-joint manipulator. J. Intell. Robot. Syst. **51**(2), 159–186 (2008)
41. Chaoui, H., Gueaieb, W., Biglarbegian, M., et al.: Computationally efficient adaptive type-2 fuzzy control of flexible-joint manipulators. Robotics **2**(2), 66–91 (2013)

42. Li, Y., Li, K., Tong, S.: Finite-time adaptive fuzzy output feedback dynamic surface control for MIMO nonstrict feedback systems. IEEE Trans. Fuzzy Syst. **27**(1), 96–110 (2019)
43. Wu, D.: Approaches for reducing the computational cost of interval type-2 fuzzy logic systems: overview and comparisons. IEEE Trans. Fuzzy Syst. **21**(1), 80–99 (2013)
44. Mohammadzadeh, A., Hashemzadeh, F.: A new robust observer-based adaptive type-2 fuzzy control for a class of nonlinear systems. Appl. Soft Comput. **37**, 204–216 (2015)
45. Bibi, Y., Bouhali, O., Bouktir, T.: Petri type 2 fuzzy neural networks approximator for adaptive control of uncertain non-linear systems. IET Control Theory Appl. **11**(17), 3130–3136 (2017)
46. Liu, X., Yang, C., Chen, Z., et al.: Neuro-adaptive observer based control of flexible joint robot. Neurocomputing **275**, 73–82 (2018)